CFD prediction of flowfield and snowdrift around building complex in snowy region

Yoshihide Tominaga and Akashi Mochida

Niigata Institute of Technology, Kashiwazaki-shi, Fujihashi 1719, 945-1195, Japan

Abstract

A CFD (Computational Fluid Dynamics) technique is applied to the prediction of snowdrift around a 9-storey apartment building. A modified version of the Launder-Kato type k-ε model (LK model[5,9,10]) is used. In the first part of the paper, results of a preliminary study for a flowfield around a cube placed in a channel flow are presented. Here, results obtained by using the modified LK model are compared with those of measurements and the standard k-ε model. The latter part describes the numerical prediction of snowdrift around a 9-storey apartment building which is presently under construction in Nagaoka City, Niigata Prefecture. Special emphasis is given to snowdrift into elevator hall.

1. Introduction

Snowdrift significantly affects human activities in snowy regions. Many experimental studies have been carried out using wind tunnel technique to predict snowdrift around buildings[1,2]. However, it is very difficult in some cases to satisfy the similarity requirements for wind tunnel studies on snowdrift. Furthermore, wind tunnel equipment is not readily available to many planners, designers, etc. Thus, a numerical method for predicting snowdrift is expected to become a useful tool for architectural design and city planning in snowy regions.

In this paper, a three-dimensional numerical method using a modified version of the Launder-Kato type k-ε model (modified LK model)[5,9,10] coupled with the transport equation of snowdrift density is applied to the prediction of snowdrift around a building. Here, the accuracy of the modified LK model is examined for a flowfield around a cube placed within a channel flow before conducting the snowdrift prediction. Next, the numerical predictions of flow over a building complex in Nagaoka City, Niigata Prefecture, and snowdrift around an apartment building are conducted using the modified LK model.

2. Outline of numerical method

2.1 Flowfield analyzed

Fig. 1 illustrates a 9-storey apartment building site. The surrounding area is mostly covered by low-rise residential houses. Fig.2 shows a horizontal plan of the building. The wind break screen made of glass, which is expected to intercept the snow particles coming directly from the NNE direction, is installed in front of the elevator hall.

2.2 Computational domain and grid arrangements

In this study, two types of computations were conducted on two different grid systems : grid A and grid B. Grid A covers the whole computational domain (region A shown in Fig.1; 198m (x_1) × 178m(x_2) × 100m(x_3)) . The entire flow pattern is predicted

by the prediction based on grid A. Grid B is applied to the region near the analyzed building (region B, 21m (x_1) × 16m (x_2) × 28m(x_3), indicated in Fig.2). The detailed distributions of velocity vectors and snowdrift density are predicted in region B using grid spacings which are much finer than those for region A. The boundary conditions on the surface of region B are obtained by interpolating the predicted results in region A. Region A is discretized into 70(x_1) × 70(x_2) × 34(x_3), while the region B is divided into 57 (x_1) × 51 (x_2) × 29(x_3) grids.

2.3 Computed cases

Two prediction cases, with and without a glass screen installed in the elevator hall as a wind break (cf. Fig.2), are carried out to investigate its effects.

2.4 Turbulence model

There are many difficulties in predicting the complex turbulent flow field around a bluff body such as a building using a standard k-ε model[4]. The standard k-ε model is not suitable for predicting a flowfield that includes impinging, separation, etc. Therefore, this model cannot reproduce well wind velocity near the front corners of a building. This is because the standard k-ε model overestimates production P_k of turbulence kinetic energy k, around the front corners.

Launder and Kato[5] proposed a revised k-ε model (hereafter denoted as LK model) which eliminates the excessive production of k around a stagnation point, by modifying the expression for P_k. The LK model expresses P_k, as a function of S and Ω (eq.(4) in Table 1, S is the strain rate scale, Ω is the vorticity scale) to eliminate the excessive production of k.

This model corrects the overestimation of k around the impinging region. However, in the flowfield where Ω/S>1, the expression for P_k in eq.(4) overestimates P_k compared to that for the standard k-ε model expressed as eq.(1) in Table 1. To avoid this overestimation, eq.(4) must be utilized for the LK model only in the region where Ω/S<1. The authors call this modification "modified LK model", and it is used in this study[9,10].

2.5 Model for suspension of snow particles

Transport of snow particles consists of three processes : saltation, suspension and creep. The effect of suspension is very important in this study, because special emphasis is given to snowdrift into the elevator hall. Thus, only suspension of snow particles is considered in our predictions. Here, the suspension of the snow particles is predicted by using the following transport equation of snowdrift density[6].

$$\frac{\partial \Phi}{\partial t} + \frac{\partial \Phi < u_j >}{\partial x_j} + \frac{\partial \Phi W_S}{\partial x_3} = \frac{\partial}{\partial x_j}\left(\frac{\nu_t}{\sigma_S} \frac{\partial \Phi}{\partial x_j} \right), \qquad (8)$$

where Φ is the snowdrift density. W_S is the snowfall velocity and the value of 0.5m/s is selected in this study[8]. The eddy diffusion coefficient of snowdrift density is assumed to be equal to that of momentum, i.e., σ_S=1.0. Eq.(8) is similar to the transport equation for airborne particles in a clean room proposed by Murakami, Kato et al.[7]

2.6 Boundary conditions

Boundary conditions for the computation using grid A are summarized in Table 2. Computations are conducted for the wind direction NNE, and the wind velocity is

2.9m/s at 6.5m height at inflow boundary. The boundary conditions on the surface of region B are obtained by interpolating the predicted results ($<u_1>$,$<u_2>$,$<u_3>$,k,ε) for region A. Furthermore, snowdrift density Φ is set to unity for inflow boundaries of grid B. At the outflow boundaries of grid B, normal gradients of velocities, k,ε andΦ are set to zero.

3. Results and discussion

3.1 Preliminary study using the modified LK model for flow around a cube

Before conducting the simulation of flow over the actually planned complicated building, a preliminary study was conducted using the modified LK model for flowfield around a single cube placed on a channel wall. Marutinuzzi et al.[11] carried out detailed LDA measurements for this flowfield. Boundary conditions are summarized in the appendix.

Fig. 3(1) compares velocity vectors in the central vertical section obtained from the modified LK model, the standard k-ε model, with the measurement[11]. At the separation region on the roof, it can be observed that the reattachment length is severely underestimated by the standard k-ε model. However, the reattachment length on the roof becomes much longer for the modified LK model, and the result of modified LK model shows better agreement with the experiment than the standard k-ε model. This improvement reflects the significant reduction of the turbulence kinetic energy k produced in front of the cube, as can be seen from the distribution of k given in Fig 3(2). Fig.4 displays the computed and measured $<u_1>$ velocity profiles at different streamwise locations on the roof (x_1/H=0.5 and 1.0, H is the cube height). As already seen in Fig.3(1), significant differences are observed between the results of the standard k-ε model and the modified LK model on the roof. The results given by the modified LK model show better agreement with the experiments. It was confirmed here that the modified LK model provided better results than the standard k-ε model for flowfield around a cube. In the next section, the modified LK model is applied to the prediction of flow over the building complex in Nagaoka City and snowdrift around the 9-storey apartment building under construction.

3.2 Velocity vector over building complex (Grid A)

The predicted velocity field near ground level (x_3=1.5m) is illustrated in Fig.5(1). The shaded building is the 9-storey apartment building, and the flowfield around it is investigated here. The numerical result reproduces well the complicated flowfield near ground level. It is shown that strong gusts occur at the windward corners of the building, and a reverse flow region is formed behind the building. The velocity vector at the x-x' section is illustrated in Fig.5(2). A stagnation point in front of the building, separation at the front corner, and recirculating flow behind the building are clearly seen in this figure.

3.3 Snowdrift into the elevator hall of the apartment building(Grid B)

Fig. 6 shows the velocity vectors around the apartment building. No clear difference was observed in the overall flow patterns with and without the screen in front of the elevator hall. Thus, only the result with the screen is shown here. In vertical central section (Fig.6(1)), it is observed that the approach flow is the separated into rising flow and down flow at the building's mid-height. The velocity in the elevator hall is relatively low and the scalar velocity values are 0.1～0.2[m/s].

Distributions of snowdrift density are compared in Figs. 7-9. Fig. 7 illustrates

the snowdrift densities in the same section as that for Fig.6(1). The snowdrift densities in the elevator hall are 0.3～0.6 without the screen (Fig.7(1)). However, there is no invasion of snowdrift into the elevator hall with the screen (Fig.7(2)), although the density is rather large outside the screen. Distributions of snowdrift density in horizontal planes are shown in Figs. 8 and 9. Large differences are observed between the two cases. It is clearly shown that the wind break screen installed in the elevator hall effectively reduces the snowdrift density inside the hall.

4. Conclusion

1) A three-dimensional CFD method using the modified LK model coupled with the transport equation of snowdrift density was applied to the predictions of the flowfield over a building complex in Nagaoka City and snowdrift around a 9-storey apartment building.
2) Before carrying out the predictions of snowdrift, the accuracy of the numerical results obtained using the modified LK model was examined for a flowfield around a cube placed within a channel flow. The modified LK model was confirmed to provide better results than the standard k-ε model.
3) It was demonstrated that numerical simulation is a very powerful tool for analyzing snowdrift around the building actually being planned, and this provides information which is difficult to obtain by experimental techniques. By successively decreasing the computational domain, the snowdrift into elevator hall can be reproduced very well.

Appendix : Boundary conditions for flow past a cube on a channel wall

The computational domain covers $14.5H(x_1)\times 9.0H(x_2)\times 2H(x_3)$ (H is the cube height). It is discretized into $90(x_1)\times 64(x_2)\times 32(x_3)$. The minimum grid width is 0.01H. On the lower and upper boundaries of the channel and the cube walls, the generalized logarithmic law is employed. At inflow boundary, the values interpolated from the results of LES computation for fully developed channel flow at Re=40,000 conducted by Piomelli[12] are imposed as the boundary condition.

Nomenclature

x_i : three components of spatial coordinate (i=1,2,3;streamwise,lateral,vertical)
$\langle u_i \rangle$: velocity component in the x_i direction
k : turbulence kinetic energy
ν_t : eddy viscosity
ε : turbulence dissipation rate
$\langle u_t \rangle_p$: tangential velocity component at the near-wall node
h_p : mesh interval adjacent to solid wall
k_p : k value at the near-wall node

References

[1] Anno, Y.: Development of a snowdrift wind tunnel, Cold Reg. Sci. Technol., 10(2), pp153-161 (1985)
[2]Toyoda,K., Tomabechi,T.: Development of a wind tunnel for the study of snowdrifting, 2nd Intern. Conf. on Snow Eng., Santa Barbara, California (1992)
[3]Uematsu,T., Kaneda,Y., Takeuchi,K., Nakata, T. and Yukumi, M. : Numerical simulation of snowdrift development. Ann. Glaciol.,13, pp.265-267(1989)
[4]Murakami, S., Mochidaa, A. and Hayashi, Y. :Examining the k-ε model by means of a wind tunnel test and large eddy simulation of turbulence structure around a cube, J. Wind Eng. Ind. Aerodyn. 35,pp.87-100(1990)

[5]Launder,B.E., Kato, M. : Modeling flow-induced oscillations in turbulent flow around square cylinder, ASME Fluid Eng. Conference, pp20(1993)
[6]Sato,T. Uematsu,T. et al. : Three-dimensional numerical simulation of snowdrift, J. Wind Eng. Ind. Aerodyn. 46/47(1993)
[7]Murakami,S., Kato,S.,Nagano,S. and Tanaka, Y. : Diffusion characteristics of airborne particles with gravitational settling in a convection-dominant indoor flow field, ASHRAE Transactions vol.98,Pt.1,(1992)
[8]Kajikawa, M., Taniguchi, S., Ito, S.: Relationship between the fall velocity of snowflakes and the shape of their component crystals, "Seppyo", vol.58,6,pp.455-462(1996)
[9]Tsuchiya,M.,Murakami,S.,Mochida,A.,Kondo,K.,Ishida,Y. : Development of a new k-ε model for flow and pressure fields around bluff body, J. of Wind Engineering and Industrial Aerodynamics 67/68,pp169-182(1997)
[10]Kondo, K., Murakami,S.,Mochida,A.: Numerical study on flowfield around square rib using revised k- ε model, Proc. 8th Japan National Symp. on Comput. Fluid Dyn., pp.363-366(1994)(in Japanese)
[11]Murtinuzzi, R. Tropea, C. : The flow around surface-mounted prismatic obstacle placed in a fully developped channel flow, J. Fluids Eng. 115,pp.85-92 (1993)
[12]Piomelli, U. : High Reynolds number calculations using the dynamic subgrid-scale stress model, Phys.Fluids, A5(6)pp.1484-1490(1993)

Table 1　Model equations (expressions for P_k and ν_t)

1. Standard k-ε model

$$P_k = \nu_t S^2 \quad (1) \qquad \nu_t = C_\mu \frac{k^2}{\varepsilon} \quad (2) \qquad S = \sqrt{\frac{1}{2}\left(\frac{\partial <u_i>}{\partial x_j} + \frac{\partial <u_j>}{\partial x_i}\right)^2} \quad (3)$$

2. LK model

$$P_k = \nu_t S\Omega \quad (4) \qquad (\nu_t : \text{eq.(2)}) \qquad \Omega = \sqrt{\frac{1}{2}\left(\frac{\partial <u_i>}{\partial x_j} - \frac{\partial <u_j>}{\partial x_i}\right)^2} \quad (5)$$

3. Modified LK model

$P_k = \nu_t S^2$　($\Omega/S>1$)　(6)

$P_k = \nu_t S\Omega$　($\Omega/S \leqq 1$)　(7)

Table 2 boundary condition for the computation using grid A

Inflow	$<u_1(x_3)> \propto x_3^{1/4}$ (at 6.5m height, $<u_1>$=2.9m/s) $<u_2(x_3)> = <u_3(x_3)> = 0$ $k(x_3)$ = constant value = 0.08[m²/s²] (estimated from the relation that $k = C_\mu^{-1/2} u_*^2$) $\ell(x_3) = (C_\mu k(x_3))^{1/2} (\partial <u_1(x_3)> / \partial x_3)^{-1}$ (at inflow boundary, we assume $P_k = \varepsilon$) $\varepsilon(x_3) = C_\mu k(x_3)^{3/2} / \ell(x_3)$, $\nu_t(x_3) = k(x_3)^{1/2} / \ell(x_3)$
Outflow	$<u_i>$, k, ε : $\partial / \partial x_n = 0$ (x_n : spatial coordinate normal to the boundary plane)
Upper face of computational domain	$<u_3>=0$, $<u_1>$, $<u_2>$, k, ε : $\partial / \partial x_3 = 0$
Ground	$\frac{<u_t>_P}{u_*} = \frac{1}{\kappa} \ln \frac{1/2 h_P}{z_0}$, $\bar{\varepsilon} = \frac{u_*^3}{\kappa h_P} \ln \frac{h_P}{z_0}$, $\varepsilon_P = \frac{C_\mu^{3/4} k_P^{3/2}}{1/2 \kappa h_P}$
Building wall	$\frac{<u_t>_P}{u_*} (C_\mu^{1/2} k_P)^{1/2} = \frac{1}{\kappa} \ln \left[E \frac{1}{2} h_P (C_\mu^{1/2} k_P)^{1/2} / \nu \right]$ $\bar{\varepsilon} = \frac{C_\mu^{3/4} k_P^{3/2}}{\kappa h_P} \ln \left[E h_P (C_E^{1/2} k_P)^{1/2} / \nu \right]$ κ=0.4, C_μ=0.09, E=9.0, h_P=0.5m, z_0=0.3m

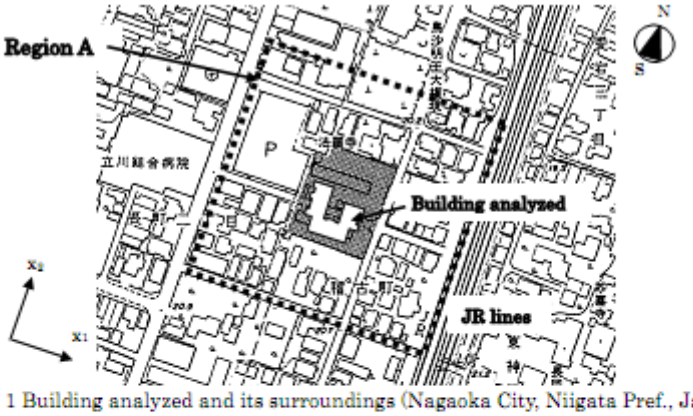

Fig. 1 Building analyzed and its surroundings (Nagaoka City, Niigata Pref., Japan)

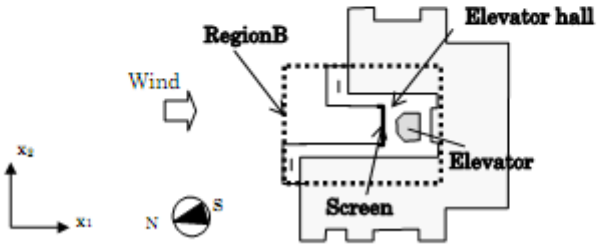

Fig. 2 Horizontal plan of the building

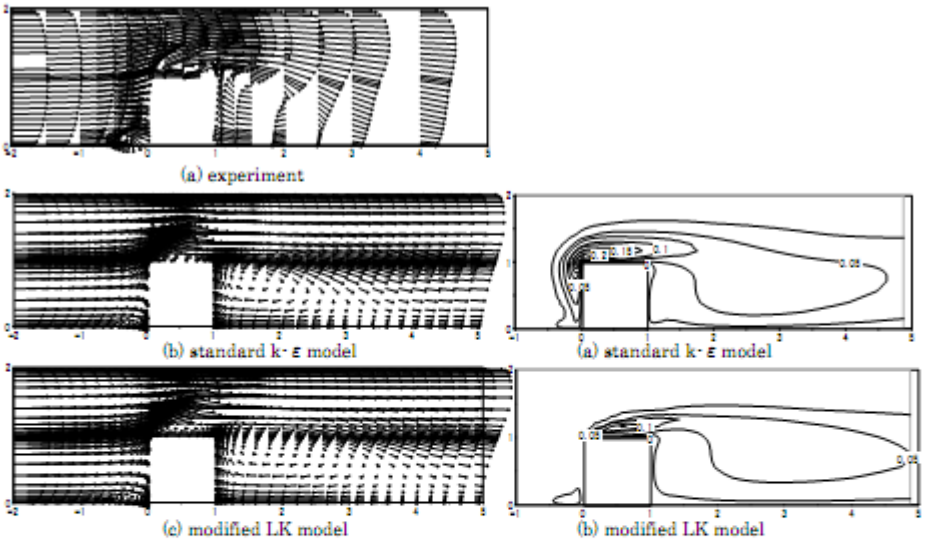

(1) Velocity vectors (2) Turbulence kinetic energy k

Fig.3 Comparison of velocity vectors and k for flow around a cube (in center section)

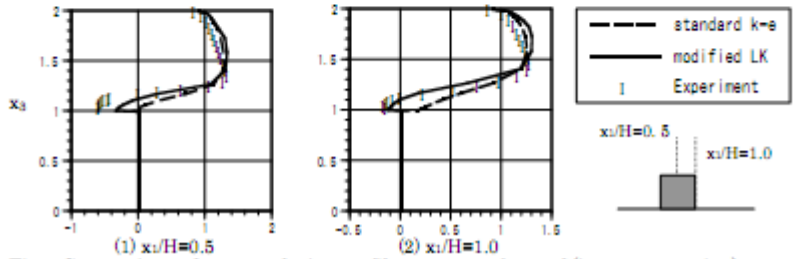

Fig.4 Comparison of mean velocity profiles <u_1> on the roof (in center section)

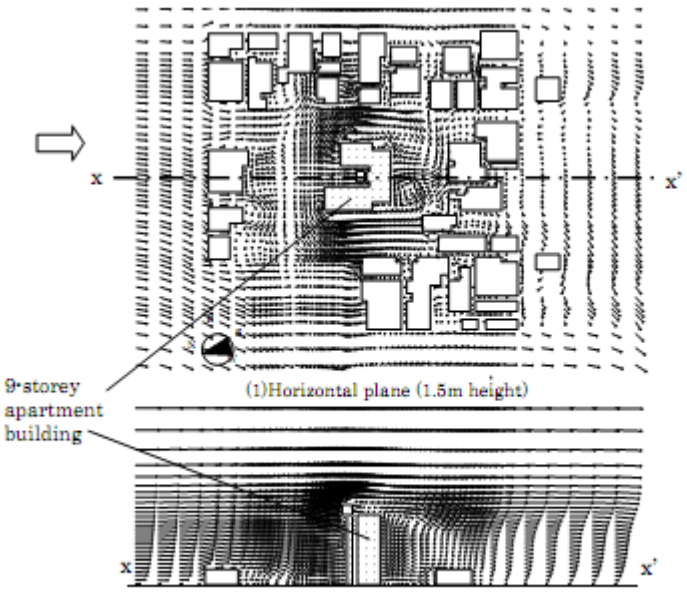

(1)Horizontal plane (1.5m height)

(2)Vertical plane (x-x' section)

Fig.5 Velocity vectors (Region A)

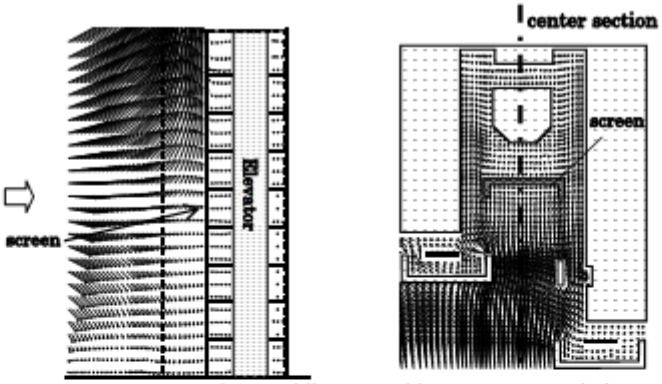

(1) Center section (cf. Fig.6(2)) (2) Horizontal plane (9F)

Fig.6 Velocity vectors (with screen)

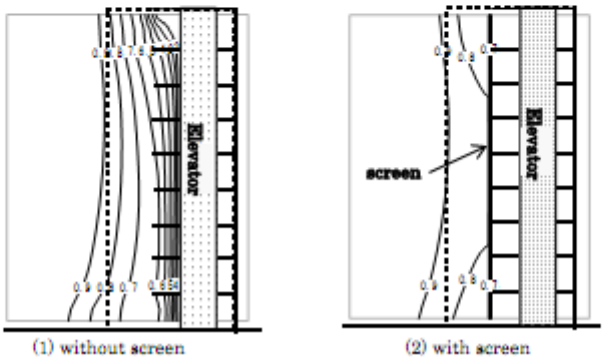

(1) without screen (2) with screen

Fig.7 Snowdrift density in center section

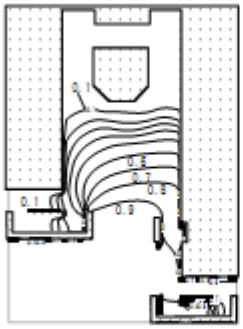

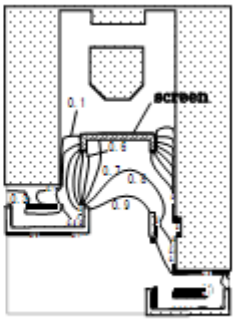

(1) without screen　　(2) with screen

Fig.8　Snowdrift density（9F: Horizontal plane）

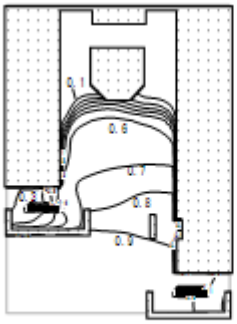

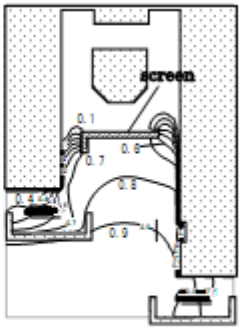

(1) without screen　　(2) with screen

Fig.9　Snowdrift density（1F: Horizontal plane）